



## Epitools, a software suite for presurgical brain mapping in epilepsy : Intracerebral EEG

Samuel Medina Villalon, Rodrigo Paz, Nicolas Roehri, Stanislas Lagarde,  
Francesca Pizzo, Bruno Colombet, Fabrice Bartolomei, Romain Carron,  
Christian-G. Bénar

### ► To cite this version:

Samuel Medina Villalon, Rodrigo Paz, Nicolas Roehri, Stanislas Lagarde, Francesca Pizzo, et al..  
Epitools, a software suite for presurgical brain mapping in epilepsy : Intracerebral EEG. Journal of  
Neuroscience Methods, 2018, 10.1016/j.jneumeth.2018.03.018 . hal-01762672

**HAL Id: hal-01762672**

**<https://hal.science/hal-01762672>**

Submitted on 10 Apr 2018

**HAL** is a multi-disciplinary open access archive for the deposit and dissemination of scientific research documents, whether they are published or not. The documents may come from teaching and research institutions in France or abroad, or from public or private research centers.

L'archive ouverte pluridisciplinaire **HAL**, est destinée au dépôt et à la diffusion de documents scientifiques de niveau recherche, publiés ou non, émanant des établissements d'enseignement et de recherche français ou étrangers, des laboratoires publics ou privés.

# **EpiTools, A software suite for presurgical brain mapping in epilepsy:**

## **Intracerebral EEG.**

S Medina Villalon<sup>1,2</sup>, R Paz<sup>3+</sup>, N Roehri<sup>1+</sup>, S Lagarde<sup>1,2</sup>, F Pizzo<sup>1</sup>, B Colombet<sup>1</sup>, F Bartolomei<sup>1,2</sup>, R

Carron<sup>1,4</sup>, C-G Bénar<sup>1\*</sup>

- 1) Aix Marseille Univ, Inserm, INS, Inst Neurosc Syst, Marseille, France
- 2) APHM, Timone Hospital, Clinical Neurophysiology, Marseille, France
- 3) IFIBIO Bernardo Houssay, Grupo de Neurociencia de Sistemas, Facultad de Medicina, Universidad de Buenos Aires-CONICET, 2155 Paraguay Street, Buenos Aires 1121, Argentina
- 4) APHM, Timone Hospital, Functional and stereotactic neurosurgery, Marseille, France

+ equally contributing authors

\* corresponding author

Tel +33 (0)4 91 38 55 62

e-mail : [christian.benar@univ-amu.fr](mailto:christian.benar@univ-amu.fr)

Institut de Neurosciences des Systèmes-UMR 1106,

Faculté de Médecine La timone, 27 bd Jean Moulin 13005 Marseille

## **Abstract**

### **Background**

In pharmacoresistant epilepsy, exploration with depth electrodes can be needed to precisely define the epileptogenic zone. Accurate location of these electrodes is thus essential for the interpretation of Stereotaxic EEG (SEEG) signals. As SEEG analysis increasingly relies on signal processing, it is crucial to make a link between these results and patient's anatomy.

Our aims were thus to develop a suite of software tools, called "EpiTools", able to i) precisely and automatically localize the position of each SEEG contact and ii) display the results of signal analysis in each patient's anatomy.

### **New Method**

The first tool, GARDEL (GUI for Automatic Registration and Depth Electrode Localization), is able to automatically localize SEEG contacts and to label each contact according to a pre-specified nomenclature (for instance that of FreeSurfer or MarsAtlas). The second tool, 3Dviewer, enables to visualize in the 3D anatomy of the patient the origin of signal processing results such as rate of biomarkers, connectivity graphs or Epileptogenicity Index.

### **Results**

GARDEL was validated in 30 patients by clinicians and proved to be highly reliable to determine within the patient's individual anatomy the actual location of contacts.

### **Comparison with Existing Methods**

GARDEL is a fully automatic electrode localization tool needing limited user interaction (only for electrode naming or contact correction). The 3Dviewer is able to read signal processing results and to display them in link with patient's anatomy.

### **Conclusion**

EpiTools can help speeding up the interpretation of SEEG data and improving its precision.

## Keywords

Epilepsy, SEEG, automatic segmentation, contacts localization, 3D rendering, CT.

### 1. Introduction

About one third of patients with epilepsy are refractory to medical treatment (Kwan and Brodie, 2000). Some of them suffer from focal epilepsy; for these patients, epilepsy surgery is an efficient option (Ryvlin et al., 2014). The goal of epilepsy surgery is to remove the epileptogenic zone (EZ), i.e., the structures involved in the primary organization of seizures, and to spare the functional cortices (e.g. involved in language or motor functions). For this purpose, a pre-surgical work-up is needed including a non-invasive phase with clinical history and examination, cerebral structural and functional imaging (MRI and PET), neuropsychological assessment and long-term surface EEG recordings. Nevertheless, for about one quarter of these patients, it is difficult to correctly identify the EZ and/or its relationship with functional areas. For these difficult cases, an invasive study with intracranial EEG is required (Jayakar et al., 2016). Stereo-EEG (SEEG) is a powerful method to record local field potentials from multiple brain structures, including mesial and subcortical structure. It consists in a stereotaxic surgical procedure performed under general anesthesia and aiming at implanting 10 to 20 electrodes within the patient's brain. Each electrodes being made up of 5 to 18 contacts, (McGonigal et al., 2007), (Cossu et al., 2008).

SEEG allows high resolution mapping of both the interictal, i.e. between seizures, and ictal activity, and helps delineate the epileptic network, determine which specific areas need to be surgically removed (Bartolomei et al., 2008), and identify the functional regions to be spared (Trébuchon-Da Fonseca et al., 2005). The SEEG interpretation crucially relies on combined use of three sources of information: clinical findings, anatomy and electrophysiology. Therefore, it is of utmost importance to precisely localize the origin of the SEEG signal within the patient's anatomy, as was done in the field of EcoG (Dykstra et al., 2012), (Groppe et al., 2017).

The intracerebral position of SEEG electrodes is usually assessed visually by clinicians, based on the

registration of MRI scan on CT image. However, this approach is time consuming (100 to 200 contacts by patients) and a potential source of error. The use of a software allowing automatic localization of electrodes contact within the patient's MRI would thus be very helpful. Such software should be able to perform: i) an automatic and optimal localization of contact positions with respect to each patient's cerebral anatomy, ii) an automatic labelling of the SEEG contacts within an individualized atlas. Currently, there isn't any software available to perform automatically such processes. Indeed, previous studies have proposed semi-automatic registration of intracranial electrodes contacts, based on Computerized tomography (CT) and Magnetic resonance imaging (MRI) images and prior information such as planned electrodes trajectory (Arnulfo et al., 2015), (Narizzano et al., 2017) or manual interactions (Princich et al., 2013), (Qin et al., 2017).

On the other hand, advances in signal analysis (including connectivity) of epileptic activities in SEEG have been major in recent years and now constitute key factors in the understanding of epilepsy (Bartolomei et al., 2017). The translation of such advanced analyses to clinical practice is challenging but should lead to improvement in SEEG interpretation. Therefore, there is a need to easily apply some signal analysis to raw SEEG signal and then to graphically display their results in the patient's anatomy.

Our objective was thus to design a suite of software tools, with user-friendly *graphical user interfaces* (GUIs), which enables to i) identify with minimal user input the location of SEEG contacts within individual anatomy ii) label contacts based on a surface approach as implemented in FreeSurfer (Fischl, 2012) or MarsAtlas (Auzias et al., 2016) iii) interact with our in-house AnyWave software (Colombet et al., 2015) and associated plugins in order to display signal processing results in the patient's MRI or in a surface rendering of the patient's cortex. Hereafter, we will describe step by step the implementation of our suite "EpiTools". The suite as well as the full documentation are freely available on our web site <http://meg.univ-amu.fr/wiki/GARDEL:presentation>. It includes mainly the following software programs: GARDEL (for "GUI for Automatic Registration and Depth Electrodes Localization"), the 3Dviewer for 3D visualization of signal processing results within the AnyWave framework.

## 2. Material and Methods

The complete pipeline is illustrated in **Fig.1**. Firstly, FreeSurfer pipeline (1) can be run optionally on MRI image to obtain pial surface and Atlases. Then, “GARDEL” (2) tool was developed to co-register MRI on CT scan, detects automatically SEEG contacts and label them if an atlas is available. It saves electrodes coordinates to be reused. Finally, the “3Dviewer” (4) tool is designed to display signal analysis results, obtained thanks to “AnyWave” (3) and attached plugins, inside patient individual brain mesh or MRI slices. Inputs are : i) MR pre-implantation and CT post-implantation images, ii) if needed, results of FreeSurfer pipeline (Pial surface and Atlases) (Fischl, 2012) or MarsAtlas (Auzias et al., 2016), iii) SEEG electrophysiological signal processing results. The output consists of a 3D visualization of these data in the patient’s own anatomical rendering, a selection of SEEG contacts found inside grey matter for signal visualization in AnyWave software and brain matter or label associated with each contact. The different tools of our pipeline are written in Matlab (Mathworks, Natick, MA), and can be compiled to be used as standalone in all operating systems (requiring only the freely available Matlab runtime).

### 2.1 SEEG and MRI data

In our center, SEEG exploration is performed using intracerebral multiple-contact electrodes (Dixi Medical (France) or Alcis (France): 10–18 contacts with length 2 mm, diameter 0.8 mm, and 1.5 mm apart; for details see (Bartolomei et al., 2008)). Some electrodes include only one group of contacts regularly spaced (5,10, 15 and 18 contacts per electrode), and others are made up of 3 groups of 5 or 6 contacts spaced by 7-11 mm (3x5 or 3x6 contacts electrodes). There are two types of electrodes implantation: orthogonal and oblique. Electrodes implanted orthogonally are almost orthogonal to the sagittal plane and almost parallel to the axial and coronal planes. Electrodes implanted obliquely can be implanted with variable angle. The choice of the type and number of electrodes to be implanted depends on clinical needs. Intracerebral recordings were performed in the context of their pre-surgical evaluation. Patients signed informed consent, and the study was approved by the Institutional Review

board (IRB00003888) of INSERM (IORG0003254, FWA00005831).

All MR examinations were performed on a 1.5 T system (Siemens, Erlangen, Germany) during the weeks before SEEG implantation. The MRI protocol included at least T1-weighted gradient-echo, T2-weighted turbo spin-echo, FLAIR images in at least two anatomic planes, and a 3D-gradient echo T1 sequence after gadolinium based contrast agents (GBCA) injection. Cerebral CT (Optima CT 660, General Electric Healthcare, 120 kV, 230-270 FOV, 512x512 matrix, 0.6mm slice thickness), without injection of contrast agents, were performed the day after SEEG electrodes implantation. Each CT scan was reconstructed using the standard (H30) reconstruction kernel to limit the level of streaks or flaring.

## **2.2 The AnyWave framework**

Our tools GARDEL and the 3Dviewer are intended to interact with the AnyWave<sup>1</sup> software, developed in our institution for the visualization of electrophysiological signals and for subsequent signal processing (Colombet et al., 2015). AnyWave is multi-platform and allows to add plugins created in Matlab or Python<sup>2</sup>. Some specific plugins were created and added to implement measure for SEEG analysis as Epileptogenicity Index (EI) (Bartolomei et al., 2008), non-linear correlation  $h^2$  (Wendling et al., 2001), Interictal spikes or high frequency oscillations (HFO) detections (Roehri et al., 2017, 2016) as well as graph measures (Courstens et al., 2016).

## **2.3 Electrode contact segmentation and localization**

GARDEL localizes the SEEG contacts in the patient's anatomy. Unlike most existing techniques (Arnulfo et al. 2015; Narizzano et al. 2017; Princich et al. 2013; Qin et al. 2017), it relies on an automatic segmentation of each contact. Minimal user intervention is required (only for attributing the electrode names). It also labels each individual contact with respect to a chosen atlas (Desikan-Kiliany (Desikan et al., 2006), Destrieux (Destrieux et al., 2010), or in particular MarsAtlas (Auzias et al., 2016)).

---

<sup>1</sup> Available at [meg.univ-amu.fr](http://meg.univ-amu.fr)

<sup>2</sup> Available at <https://www.python.org/>

GARDEL takes as input a post-implantation CT-scan (where the SEEG contacts are visible as hyper density signals areas) and an anatomical MRI Volume. DICOM, NIFTI or Analyze formats are accepted. Classically, clinical images are in the DICOM format, and are converted into a NiftI format for easier manipulation, using a DICOM to NiftI converter<sup>3</sup> that can be launched within GARDEL. Image opening is made thanks to Jimmy Shen ("Tools for NiftI and ANALYZE image") toolbox<sup>4</sup>.

Since MRI and CT images have different resolution, size and origin, spatial alignment and registration are performed. In order to maintain the good quality of the CT image and keep an optimal visualization of electrodes, it was preferred to register the MRI to the CT space. The MRI is registered using maximization of Normalized Mutual Information and resliced into the CT space using a trilinear interpolation, thanks to the SPM8<sup>5</sup> toolbox (Penny et al., 2006).

With both images co-registered in the same space, the next step is to segment the electrodes on the CT scan. To do so, the resliced MRI is segmented into 3 regions: white matter, grey matter and cerebrospinal fluid using SPM (`spm_preproc` function). These three images are combined into a mask that enables us to remove extra-cerebral elements such as skull and wires (`spm_imcalc` function).

In order to segment the electrodes, a threshold is found from the histogram of grey values of the masked CT image. Electrode intensity values being significantly greater than brain structures (Hebb and Poliakov, 2009), they are defined as outliers, with a threshold based on median and quartiles :  $Thr = (Q_3 + 1.5 * IQR)$  with  $Q_3$  third quartile and  $IQR$  inter-quartile range ( $Q_3 - Q_1$ ) and could also be adjusted. The electrode segmentation is divided into 2 steps. The first step aims at segmenting each electrode individually and the second step aims at separating each contact of a given electrode. Thus, once the CT images have been thresholded, the resulting binary image is dilated using mathematical morphology (MATLAB Image Processing Toolbox, `imdilate` function) in order to bind the contacts of the same electrode together. We then find each connected component, which corresponds to each

---

<sup>3</sup> Available at <http://fr.mathworks.com/matlabcentral/fileexchange/42997-dicom-to-nifti-converter--nifti-tool-and-viewer>

<sup>4</sup> Available at <https://fr.mathworks.com/matlabcentral/fileexchange/8797-tools-for-nifti-and-analyze-image>

<sup>5</sup> Available at <http://www.fil.ion.ucl.ac.uk/spm/>



electrode, and label them separately (*bwconncomp* function) (**Fig.2a**). This results in one mask per electrode. These masks are iteratively applied to the non-dilated thresholded CT to obtain a binary image of the contacts. We then apply a distance transform of the binary image preceding a watershed segmentation (Meyer, 1994) (Matlab watershed function).

A first issue is that the watershed technique may oversegment some contacts, i.e. identify several contacts instead of one, or may miss some contacts because the contacts were too small or removed after thresholding. To solve this issue, we calculated the distance between contacts within each electrode as well as their individual volume. We removed the outliers of each feature and reconstructed the missing contacts by building a model of the electrode using the median distance and the direction vector of the electrode. The vector is obtained by finding the principal component of the correctly segmented contacts. If contacts are missed between consecutive contacts, i.e. if the distance between two consecutive contacts is greater than the median, it is divided by the median to estimate the number of missing contacts, which are then placed on the line formed by the two contacts, equally spaced. If contacts are missed at the edge of the electrode, we place contacts at the median distance of the last contact on the line given by the direction vector until the electrode mask is filled. This method allows adding missing contacts within or at the tip of the electrode. It could add contacts inside the guide screw, if it belongs to the electrode mask, but can easily be deleted after a quick review. This method enables reconstructing electrodes even if they are slightly bent, and the error made during the reconstruction of missing contacts are minimized using piece-wise linear interpolation (in contrast with simple linear interpolation) (**Fig.2b**).

A second issue is the segmentation of the 3x5 or 3x6 contacts electrodes, which are classically detected as 3 different electrodes. This is solved in two steps. Firstly, for each 5 or 6 contacts electrode, their direction vector is calculated. We then compute a dot product between them to check if they are collinear and group them. Secondly, only on these subsets of electrodes, dot products between a vector of a given electrode and vectors constructed with a point of this electrode and points of other electrodes are calculated to check if they need to be grouped.

A third issue is the difficulty to segment oblique electrodes because of the CT resolution that is not high enough in the vertical direction. To solve it, a second method for contact localization is applied after the fully automatic one, based on pre-defined electrodes characteristics (we have built in templates for Alcis and DIXI electrodes used in our center). The directions of clustered electrodes that failed the previous step are obtained by finding the principal component of each point composing these electrodes. Then, based on these electrodes characteristics and the estimated size of the clustered electrodes, a match is made and the electrodes can be reconstructed. **Fig.2c** displays the end of the segmentation process. Electrodes are projected on the maximum intensity projection image of the CT scan.

After the automatic segmentation, the user has the possibility to delete and/or add manually electrodes and/or single contacts. In order to create an electrode, the user has to mark the first contact, as well as another one along the electrode, and to choose the electrode type. This electrode will be created with respect to pre-defined electrodes characteristics (number of contacts, contact size and spacing). In order to manually correct contact position, contacts can be deleted or added one by one. Contacts numbers will be reorganized automatically.

Another important feature of GARDEL is the localization of each contact within patients' anatomy. As manual localization is usually time consuming, our goal is to localize precisely and to label automatically each contact in the brain and in individualized atlases. Atlases from FreeSurfer (Desikan-Killiany (Desikan et al., 2006) or Destrieux (Destrieux et al., 2010)) or "MarsAtlas" (Auzias et al., 2016) can be imported after having performed a transformation from FreeSurfer space to the native MRI space. For each contact, its respective label and those of its closest voxels neighbors (that formed a 3x3x3 cube) are obtained. In case of multiple labels in this region of interest, the most frequent one is used to define contact label. GARDEL provides for each SEEG contact its situation within the grey and white matter and its anatomical localization based on this atlas.

At the end, contacts coordinates, their situation within cerebral grey or white matter and anatomical

labels can be saved, for later use in the 3Dviewer (see below). GARDEL also saves automatically AnyWave montages (selection of contacts located inside grey matter and grouped them by area (frontal, occipital, parietal, temporal) for visualization of SEEG signals in AnyWave software).

**Fig.3** displays output rendering of GARDEL tool. It is possible to display electrode in patient anatomy (**Fig.3a**), in an atlas (**Fig.3b**) or all electrodes in a surface rendering of the cortex (**Fig.3c**).

## 2.4 3D representation (3Dviewer)

3Dviewer tool, closely linked to GARDEL, permits to display in a 3D way a series of relevant information inside individual mesh of the cortex:

- SEEG electrodes,
- mono-variate values such as the Epileptogenicity Index, spike or high frequency oscillation rate,
- bi-variate values such as non-linear correlation  $h^2$  or co-occurrences graph.

Data required for this tool are the following: patient's MRI scan, electrodes coordinates as given by GARDEL, pial surface made by FreeSurfer or cortex mesh made by any other toolbox (e.g. SPM), and mono-variate or bi-variate values based on format created by AnyWave and associated plugins. The parameters to be displayed can be easily set by the user: mesh, electrodes, mono or bi-variate values. Each SEEG contact is reconstructed as a cylinder with the dimension of electrodes used. Mono-variate values can either be displayed as a sphere or a cylinder with diameter and color proportional to the values. Bi-variate values (connectivity graphs) are displayed as cylinders with diameter and color proportional to the strength of the value and an arrow for the direction of the graph. Views can be switched from 3D to 2D. In the 2D view SEEG contacts are displayed on the MRI with mono-variate values in color scale (**Fig.4a**). Values are listed as tables.

As explained above, the 3Dviewer allows the 3D visualization of several signal analysis measures obtained from AnyWave software within the patient's anatomy (**Fig.4b**). One type of measure is the quantification of ictal discharges as can be done by the Epileptogenicity Index (Bartolomei et al., 2008).

Briefly, the EI is a tool quantifying epileptic fast discharge during a seizure, based on both the increase of the high frequency content of the signal and on the delay of involvement at seizure onset. It gives for each channel a measure between 0 and 1 that can be used to assess the epileptogenicity of the underlying cortex. Typically, a threshold between 0.2 and 0.3 is used for delineating the epileptogenic zone. The results could be automatically exported as a Microsoft Excel file with numerical data.

Another type of measure comes from the interictal activity, i.e. the activity between seizures. Both spikes and high frequency oscillations (HFO) are markers of epileptic cortices, and their detection and quantification are important in clinical practice. Spikes and HFO are detected by the Delphos plugin. This detector is able to automatically detect in all channels, oscillations and spikes based on the shape of peaks in the normalized (" $Z_{H0}$ ") time-frequency image (Roehri et al., 2016, 2017). Results could be exported as histogram of spike, HFO rates and combination of these two markers. A step further, the co-occurrence of inter-ictal paroxysms could bring some information about the network organization of the spiking cortices. Co-occurrence graphs can be built using the time of detection of spikes or HFOs (Malinowska et al., 2014).

Furthermore, epilepsy also leads to connectivity changes both during and between seizures. The study of such changes is important in the understanding of seizure organization, semiology, seizure onset localization, etc. The non-linear correlation  $h^2$  is a connectivity analysis method, based on non-linear regression, usefully applied in the study of epilepsy (Wendling et al., 2001)(Bartolomei et al., 2017). It is computed within the core part of AnyWave. The results could be visualized on a graph with weighted edges, directionality and delay and could also be exported on a Matlab file in order to proceed others connectivity analyses. The GraphCompare plugin quantifies the number and the strength of links between selected contacts based on  $h^2$  results to compare , with statistical testing, the connectivity of a period of interest with that of a reference period (Courstens et al., 2016). The results are represented in form of boxplots and histograms representing: total degree and strengths of nodes, and the repartition of degree of the entire network. Statistical results are also automatically exported. Finally, graph representations of edge with significant changes could also be represented.

All these results could be imported in the 3Dviewer to be represented in the patient's anatomy.

## **2.5 Validation methodology**

We validated the two aspects of our segmentation tool. Firstly, the validity of the segmentation of SEEG contact. Detected centroids were superimposed on the CT images and clinicians assessed whether centroids were entirely within the hyper-intensity region corresponding to the contact in the CT image. We performed a multi-rater analysis in order to evaluate the inter-rater agreement (using Krippendorff's  $\alpha$  (Krippendorff, 2004)). Moreover, we compared our tool to another one (iElectrodes (Blenkmann et al., 2017)). On 3 patients we picked randomly 20 contacts detected by the two software applications and calculated the mean distance between their round voxels coordinates in the CT space.

Secondly, the validation of anatomical labels. The expert neurosurgeon verified if the label assigned to each contact was concordant with the true location of the contact in the anatomy. It was labelled as "good" if it was within the right anatomical region, as "uncertain" if it was at the boundary between 2 areas and as "wrong" if it was discordant with the region it assigned.

## **3. RESULTS and DISCUSSION**

### **3.1 Validation of electrodes Segmentation**

Manual localization is time consuming. It takes in average 49 minutes for 91 contacts as explained in (Blenkmann et al., 2017) or 75 minutes for 1 implant segmentation as explained in (Narizzano et al., 2017). Our method takes in average 19 minutes of automated processing (including MRI to CT coregistration, brain segmentation and contact localization) by implantation for a double 1.90Ghz processor with 6 cores each and 16 GB RAM machine (the automatic segmentation process is parallelized between the available cores) added to manual corrections if needed. Thus, our method saves significant time for users.

Concerning the validation of our method, the first important step was to validate the localization of

SEEG contacts. We investigated 30 patients with 10 to 18 electrodes each, resulting in a total of 4590 contacts. The validation was made by an expert clinician (SL). The measure was the concordance of each reconstructed contact with the real contact as visualized on the native CT. Then, we estimated the sensitivity and precision of GARDEL. Sensitivity was defined as the number of good detections of contacts (true positive) divided by the total number of contacts of the patient and precision as the number of good detection of contacts over the total number of detections.

Our segmentation tool has a mean sensitivity of 97% (first quartile 98%, median and third quartile 100%) and a mean precision of 95% (first quartile 92%, median and third quartile 100%). Only a small subset of contacts was missed (129 out of 4590) and few false detections were obtained (243). The decrease in performance is mostly due to oblique electrodes that are not clearly distinguishable in some CT scans or when electrodes cross each other.

We also did a multi-rater comparison to confirm our results. We chose 3 more patients (more than 600 detections) that were validated by 3 raters. We obtained 83.1 % of inter-rater agreement using Krippendorff's alpha. Discrepancies were due to oblique electrodes. Separating electrode types, we obtained a full agreement among raters for orthogonal electrodes (477 contacts) and an alpha equal to 0.78 for obliques electrodes (130 contacts).

The comparison with another tool (iElectrodes(Blenkmann et al., 2017)) showed a mean difference of 0.59mm between round voxel coordinates obtained by the two tools. This difference could potentially be explained by rounding effect of centroid computation at the voxel level (our CT images had 0.42\*0.42\*0.63mm voxel size).

Therefore, our method appears to be efficient and can be used in clinical practice. It is automatic (except for naming electrodes), contrary to previous studies that used planned electrodes trajectory (Arnulfo et al., 2015; Narizzano et al., 2017) or manual interaction (Princich et al. 2013; Qin et al. 2017). In the few cases where there are errors, it is possible to easily correct manually the segmentation (explained in method section). Moreover, automatic contacts labelling using individualized atlas opens

accelerated and more robust interpretation of SEEG data in correlation with patient's anatomy. It is also possible to co-register post-resection MRI with electrode position to identify whether electrode sites were resected. However, such registration has to be performed with care for large resections, for which the brain tissues may have moved (Supp.Fig.1).

Nevertheless, a limitation of our tool resides in the fact that, in the current version, it requires inter-contact distance to be the same across electrodes. Indeed, to estimate the position of missing contacts, it takes the median distance between all contacts.

### **3.2 Validation of labelling from Atlases**

The second step was to validate the concordance between the obtained labels of each contact and its actual anatomical location. For this purpose, a senior neurosurgeon (RC) reviewed the data of 3 patients to check if our tool properly assigned each contact to its correct label according to a given atlas (different atlas per patient). Concordance results are the following: 534 over 598 contacts were accurately labeled (89.3%), 28 were uncertain (4.7%), i.e., contacts difficult to label automatically because of their location at the junction between two areas or between grey and white matters, and 36 (6%) were wrong. These errors were mostly due to incorrect segmentation of individual MRIs because of abnormalities/lesions, or in rare cases to a mismatch between atlas label and clinician labeling. It is to be noted that segmentation can be corrected at the level of the FreeSurfer software<sup>6</sup>. Results across patient were concordant (90%, 88% and 89%).

### **3.3 3Dviewer: representation of physiological data**

Signal processing is increasingly used for the analysis of SEEG (Bartolomei et al., 2017). The major interest of our pipeline is the possibility to represent on the patient's MRI scan the data from advanced electrophysiological signal analyses. This is the goal of the 3Dviewer. Data could be represented on the 3D mesh of the patients or MRI slices in the 3 spatial planes (**Fig.4**). This two modes of representation are complementary in SEEG interpretation making it possible not only to visualize the estimate of the

---

<sup>6</sup><https://surfer.nmr.mgh.harvard.edu/fswiki/FsTutorial/TroubleshootingData>

epileptic abnormalities on 3D but also to precisely localize them within brain structures and provide potentially useful guidance for surgical planning on 2D MRI slices.

#### **4. CONCLUSION**

In this study, we presented a suite of tools, called EpiTools, to be used for SEEG interpretation and related clinical research applications. The SEEG section of EpiTools is mainly based on 2 distinct parts. The first part, GARDEL, is designed for automatic electrode segmentation and labelling. It is, to the best of our knowledge, the first software to perform automatic segmentation, electrode grouping and contact labelling within individual atlas, needing only from the user to name electrodes and to correct results if necessary. We validated the contact detection and obtained good results both for sensitivity and precision. The second part consists of the 3Dviewer, which displays on the patient's MRI scan or on a 3D surface rendering, the results of signal processing at the contact location. It creates advanced link between individual anatomy and electrophysiological data analyses. In the future, we will present the application of EpiTools to non-invasive electrophysiological data such as EEG and MEG.

#### **Acknowledgements**

The authors wish to thank Olivier Coulon and Andre Brovelli for useful discussions on CT-MRI coregistration and MarsAtlas/Brainvisa use. We thank Dr Gilles Brun for helping with the writing of methods about CT imaging. The calculation of Krippendorff alpha for this paper was generated using the Real Statistics Resource Pack software (Release 5.4). Copyright (2013 – 2018) Charles Zaiontz. [www.real-statistics.com](http://www.real-statistics.com).

This work has been carried out within the FHU EPINEXT with the support of the A\*MIDEX project (ANR-11-IDEX-0001-02) funded by the "Investissements d'Avenir" French Gouvernement program managed by the French National Research Agency (ANR). Part of this work was funded by a joint Agence Nationale de la Recherche (ANR) and Direction Générale de l'Offre de Santé (DGOS) under grant "VIBRATIONS" ANR-13-PRTS-0011-01. Part of this work was funded by a TechSan grant from Agence Nationale de la recherche "FORCE" ANR-13-TECS-0013. F Pizzo was funded by "Bourse doctorale jeune



médecin” from Aix Marseille Université (PhD program ICN).

**Conflict of Interest:** The authors declare that they have no conflict of interest.

### **Authors' contributions**

SM and RP developed the GARDEL tool, SM developed the 3Dviewer, NR implemented the automatic contact segmentation, SL and FP validated the segmentation made by GARDEL, FP and SL helped on data management and clinical interpretation of results, BC developed AnyWave and its interactions with Matlab and Python, RC gave implantation information and validated Atlas labelling, FB provided patients data and co-supervised the implementation, CGB supervised the project.

### **References**

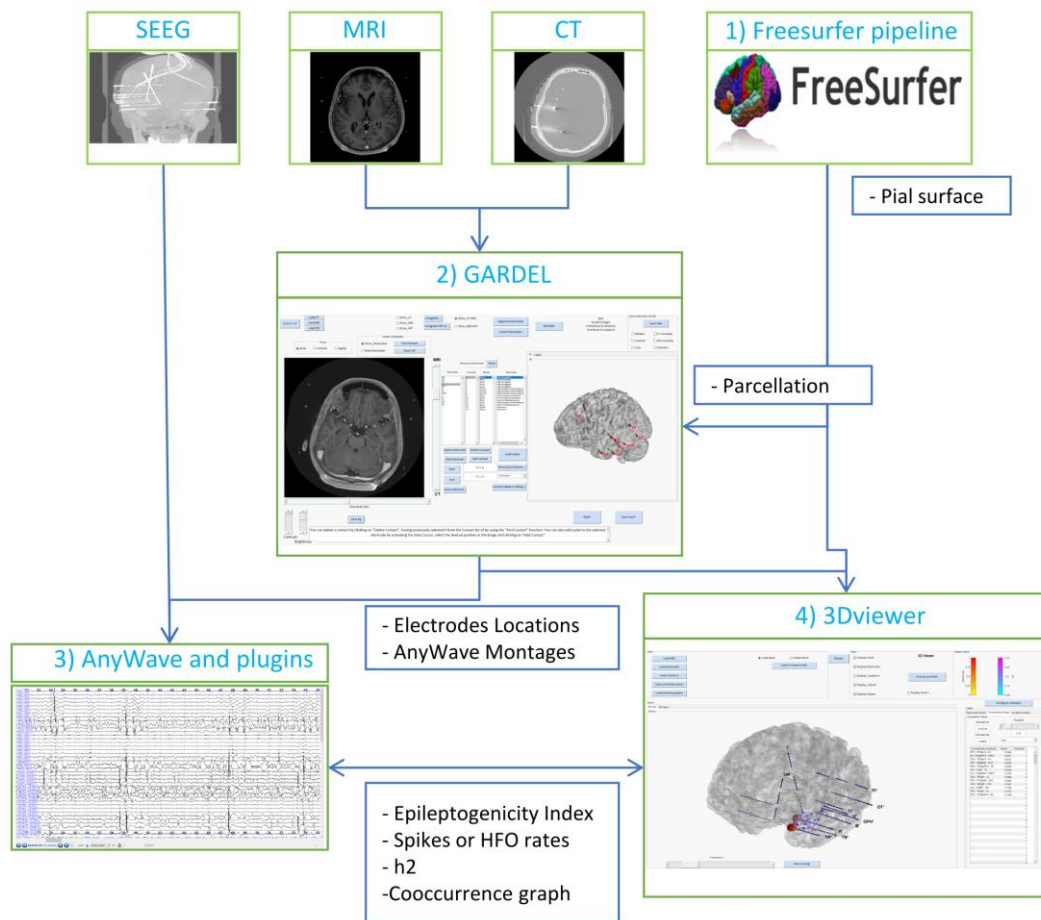
- Arnulfo, G., Narizzano, M., Cardinale, F., Fato, M.M., Palva, J.M., 2015. Automatic segmentation of deep intracerebral electrodes in computed tomography scans. *BMC Bioinformatics* 16, 12–99. <https://doi.org/10.1186/s12859-015-0511-6>
- Auzias, G., Coulon, O., Brovelli, A., 2016. MarsAtlas: A cortical parcellation atlas for functional mapping. *Hum. Brain Mapp.* 37, 1573–1592. <https://doi.org/10.1002/hbm.23121>
- Bartolomei, F., Chauvel, P., Wendling, F., 2008. Epileptogenicity of brain structures in human temporal lobe epilepsy: A quantified study from intracerebral EEG. *Brain* 131, 1818–1830. <https://doi.org/10.1093/brain/awn111>
- Bartolomei, F., Lagarde, S., Wendling, F., Mcgonigal, A., Jirsa, V., Guye, M., Bénar, C., 2017. Defining epileptogenic networks: Contribution of SEEG and signal analysis. *Epilepsia* 1131–1147. <https://doi.org/10.1111/epi.13791>
- Blenkman, A.O., Phillips, H.N., Princich, J.P., Rowe, J.B., Bekinschtein, T.A., Muravchik, C.H., Kochen, S., 2017. iElectrodes: A Comprehensive Open-Source Toolbox for Depth and Subdural Grid Electrode Localization. *Front. Neuroinform.* 11, 1–16. <https://doi.org/10.3389/fninf.2017.00014>
- Colombet, B., Woodman, M., Badier, J.M., Bénar, C.G., 2015. AnyWave: A cross-platform and modular software for visualizing and processing electrophysiological signals. *J. Neurosci. Methods* 242, 118–126. <https://doi.org/10.1016/j.jneumeth.2015.01.017>
- Cossu, M., Chabardès, S., Hoffmann, D., Lo Russo, G., 2008. Explorations préchirurgicales des épilepsies pharmacorésistantes par stéréo-électro-encéphalographie : principes, technique et complications. *Neurochirurgie* 54, 367–373. <https://doi.org/10.1016/j.neuchi.2008.02.031>
- Courtens, S., Colombet, B., Trébuchon, A., Brovelli, A., Bartolomei, F., Bénar, C.G., 2016. Graph Measures of Node Strength for Characterizing Preictal Synchrony in Partial Epilepsy. *Brain Connect.* 6, 530–539. <https://doi.org/10.1089/brain.2015.0397>

- Desikan, R.S., Ségonne, F., Fischl, B., Quinn, B.T., Dickerson, B.C., Blacker, D., Buckner, R.L., Dale, A.M., Maguire, R.P., Hyman, B.T., Albert, M.S., Killiany, R.J., 2006. An automated labeling system for subdividing the human cerebral cortex on MRI scans into gyral based regions of interest. *Neuroimage* 31, 968–980. <https://doi.org/10.1016/j.neuroimage.2006.01.021>
- Destrieux, C., Fischl, B., Dale, A., Halgren, E., 2010. Automatic parcellation of human cortical gyri and sulci using standard anatomical nomenclature. *Neuroimage* 53, 1–15. <https://doi.org/10.1016/j.neuroimage.2010.06.010>
- Dykstra, A.R., Chan, A.M., Quinn, B.T., Zepeda, R., Keller, C.J., Cormier, J., Madsen, J.R., Eskandar, E.N., Cash, S.S., 2012. Individualized localization and cortical surface-based registration of intracranial electrodes. *Neuroimage* 59, 3563–3570. <https://doi.org/10.1016/j.neuroimage.2011.11.046>
- Fischl, B., 2012. FreeSurfer. *Neuroimage* 62, 774–781. <https://doi.org/10.1016/j.neuroimage.2012.01.021>
- Groppe, D.M., Bickel, S., Dykstra, A.R., Wang, X., Mégevand, P., Mercier, M.R., Lado, F.A., Mehta, A.D., Honey, C.J., 2017. iELVis : An open source MATLAB toolbox for localizing and visualizing human intracranial electrode data. *J. Neurosci. Methods* 281, 40–48. <https://doi.org/10.1016/j.jneumeth.2017.01.022>
- Hebb, A.O., Poliakov, A. V., 2009. Imaging of deep brain stimulation leads using extended hounsfield unit CT. *Stereotact. Funct. Neurosurg.* 87, 155–160. <https://doi.org/10.1159/000209296>
- Jayakar, P., Gotman, J., Harvey, A.S., Palmieri, A., Tassi, L., Schomer, D., Dubeau, F., Bartolomei, F., Yu, A., Kršek, P., Velis, D., Kahane, P., 2016. Diagnostic utility of invasive EEG for epilepsy surgery: Indications, modalities, and techniques. *Epilepsia* 57, 1735–1747. <https://doi.org/10.1111/epi.13515>
- Krippendorff, K., 2004. Reliability in Content Analysis. *Hum. Commun. Res.* 30, 411–433. <https://doi.org/10.1111/j.1468-2958.2004.tb00738.x>
- Kwan, P., Brodie, M.J., 2000. Early identification of refractory epilepsy. *N. Engl. J. Med.* 342, 314–9. <https://doi.org/10.1056/NEJM200002033420503>
- Malinowska, U., Badier, J.M., Gavaret, M., Bartolomei, F., Chauvel, P., Bénar, C.G., 2014. Interictal networks in Magnetoencephalography. *Hum. Brain Mapp.* 35, 2789–2805. <https://doi.org/10.1002/hbm.22367>
- McGonigal, A., Bartolomei, F., Régis, J., Guye, M., Gavaret, M., Trébuchon-Da Fonseca, A., Dufour, H., Figarella-Branger, D., Girard, N., Péragut, J.C., Chauvel, P., 2007. Stereoelectroencephalography in presurgical assessment of MRI-negative epilepsy. *Brain* 130, 3169–3183. <https://doi.org/10.1093/brain/awm218>
- Meyer, F., 1994. Topographic distance and watershed lines. *Signal Processing* 38, 113–125. [https://doi.org/10.1016/0165-1684\(94\)90060-4](https://doi.org/10.1016/0165-1684(94)90060-4)
- Narizzano, M., Arnulfo, G., Ricci, S., Toselli, B., Tisdall, M., Canessa, A., Fato, M.M., Cardinale, F., 2017. SEEG assistant: a 3DSlicer extension to support epilepsy surgery. *BMC Bioinformatics* 18, 124. <https://doi.org/10.1186/s12859-017-1545-8>
- Penny, W., Friston, K., Ashburner, J., Kiebel, S., Nichols, T., 2006. Statistical Parametric

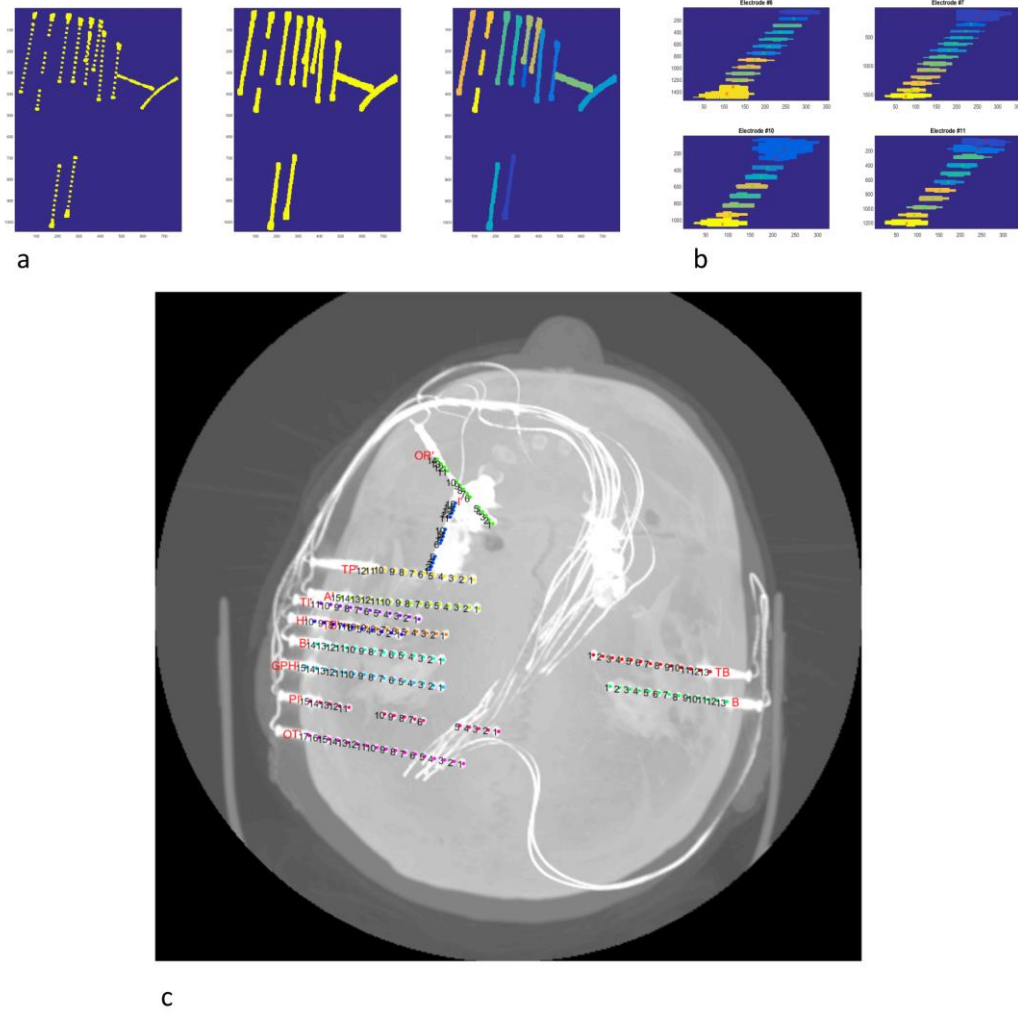
Mapping: The Analysis of Functional Brain Images. <https://doi.org/10.1016/B978-012372560-8/50002-4>

- Principich, J.P., Wassermann, D., Latini, F., Oddo, S., Blenkmann, A.O., Seifer, G., Kochen, S., 2013. Rapid and efficient localization of depth electrodes and cortical labeling using free and open source medical software in epilepsy surgery candidates. *Front. Neurosci.* 7, 1–8. <https://doi.org/10.3389/fnins.2013.00260>
- Qin, C., Tan, Z., Pan, Y., Li, Y., Ren, L., Zhou, W., Wang, L., 2017. Automatic and precise localization and cortical labeling of subdural and depth intracranial electrodes. *Front. Neuroinform.* 11, 10. <https://doi.org/10.3389/FNINF.2017.00010>
- Roehri, N., Lina, J.M., Mosher, J.C., Bartolomei, F., Benar, C.G., 2016. Time-Frequency Strategies for Increasing High-Frequency Oscillation Detectability in Intracerebral EEG. *IEEE Trans. Biomed. Eng.* 63, 2595–2606. <https://doi.org/10.1109/TBME.2016.2556425>
- Roehri, N., Pizzo, F., Bartolomei, F., Wendling, F., Benar, C.G., 2017. What are the assets and weaknesses of HFO detectors? A benchmark framework based on realistic simulations. *PLoS One* 12, 1–20. <https://doi.org/10.1371/journal.pone.0174702>
- Ryvlin, P., Cross, J.H., Rheims, S., 2014. Epilepsy surgery in children and adults. *Lancet Neurol.* 13, 1114–1126. [https://doi.org/10.1016/S1474-4422\(14\)70156-5](https://doi.org/10.1016/S1474-4422(14)70156-5)
- Trébuchon-Da Fonseca, A., Giraud, K., Badier, J.M., Chauvel, P., Liégeois-Chauvel, C., 2005. Hemispheric lateralization of voice onset time (VOT) comparison between depth and scalp EEG recordings. *Neuroimage* 27, 1–14. <https://doi.org/10.1016/j.neuroimage.2004.12.064>
- Wendling, F., Bartolomei, F., Bellanger, J.J., Chauvel, P., 2001. Interpretation of interdependencies in epileptic signals using a macroscopic physiological model of the EEG. *Clin. Neurophysiol.* 112, 1201–1218. [https://doi.org/10.1016/S1388-2457\(01\)00547-8](https://doi.org/10.1016/S1388-2457(01)00547-8)

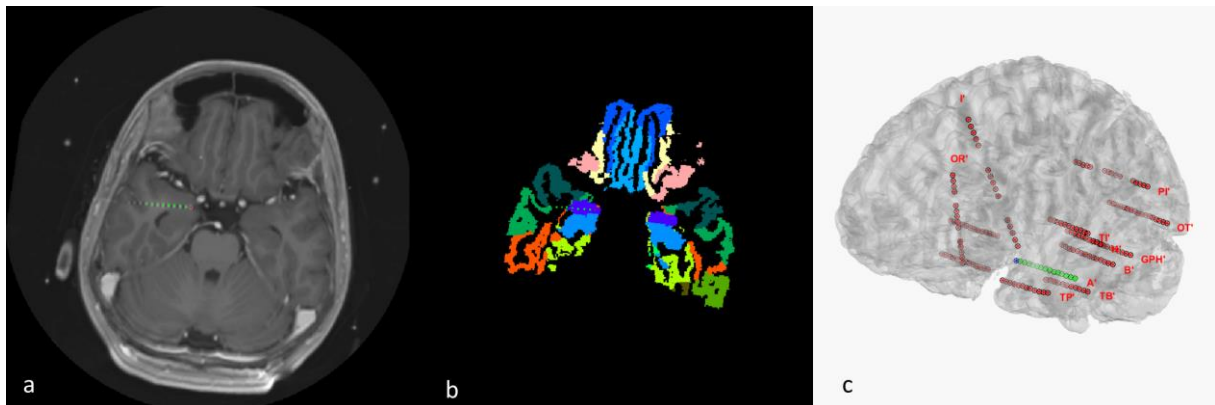
## Figure Captions



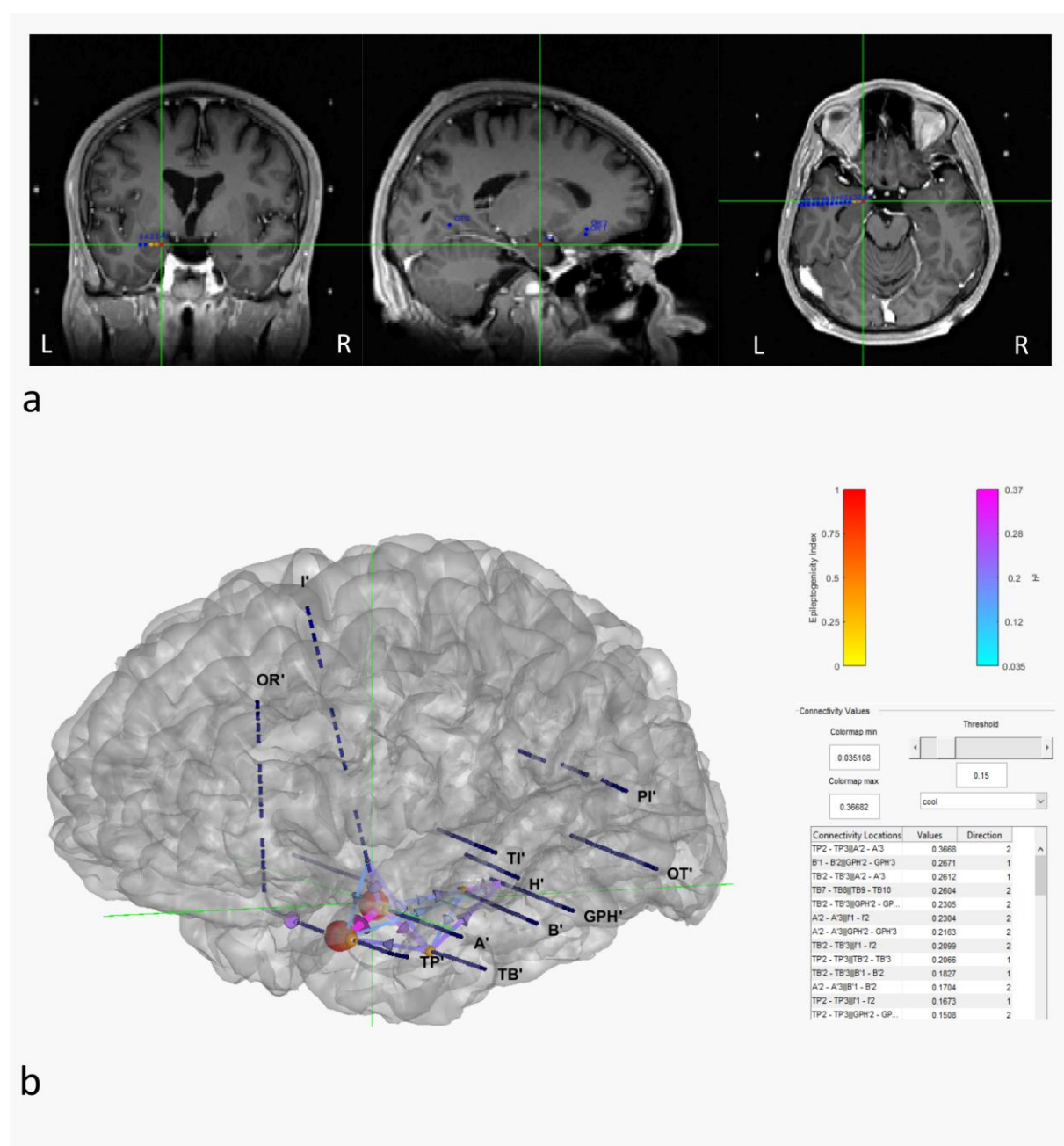
**Fig.1** Scheme of EpiTools pipeline for intracerebral EEG . Firstly, FreeSurfer(1) can be run to obtain pial surface and Atlases. Secondly, GARDEL(2) automatically localizes electrodes and contacts and labels them. Thirdly, AnyWave(3) and attached plugins are run for calculation of signal processing results and finally, the 3Dviewer(4) displays in 2D and 3D these results in MRI and patient mesh.



**Fig.2** Steps of electrodes segmentation **a)** steps of the clustering of contacts within electrodes (left panel: original image, middle panel: contacts dilated, right panel: contacts clustered within separate electrodes) **b)** Detection and reconstruction of each contact for four electrodes **c)** Final overview of the segmentation. Each image was obtained by maximum intensity projection.

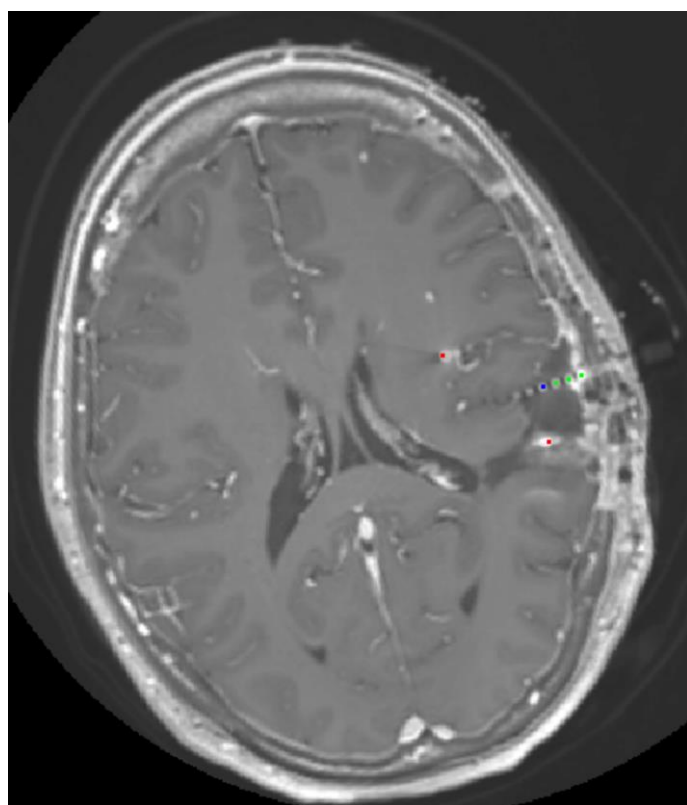


**Fig.3** Results of GARDEL tool **a)** MRI co-registered on the CT image with one electrode and its detected contacts **b)** Reconstructed electrodes inside an Atlas (in this case MarsAtlas) **c)** 3D rendering of the patient cortex with reconstructed electrodes . The centroids of each contact are displayed in these 3 figures. Electrodes are displayed in red. The selected one is displayed in green and the selected contact in blue. For clarity and match in this figure, it was displayed in red in a) and b) because of purple region of the Atlas.



**Fig.4** Overview of 3Dviewer tool results **a)** coronal, sagittal and axial planes of the patient MRI with

Epileptogenicity Index for each electrode. Each SEEG contact is displayed in blue. Epileptogenicity Index of each contact is displayed by 'hot' colormap for values above the wanted threshold. **b)** Surface rendering of the cortex showing electrodes and exemplar values for the same patient: sphere on each contact represents Epileptogenicity Index and the links between each contact represent the non-linear correlation ' $h^2$ ' calculated during a period of interest. The green cross enable matching the locations between 2D and 3Dview.



**Supp.Fig.1** Registration of contacts with post-resection MRI